Journal of

Cardiology and Therapy

Online Submissions: http://www.ghrnet.org/index./jct/
doi:10.6051/j.issn.2309-6861.2015.02.68

Journal of Cardiol Ther 2015 April 2(2): 291-301
ISSN 2309-6861(print), ISSN 2312-122X(online)

ORIGINAL ARTICLE

Upregulation of Heme Oxygenase-1 Attenuates Ischemic Heart Myocyte Cell Death and Improves Heart Function in Immunosuppressed Mice

Komal Sodhi, Paola Pesce, Sarah Stevens, Morghan Getty, Nitin Puri, Gaia Favero, Rita Rezzani, Rebecca Hutcheson, David Sacerdoti, Joseph I Shapiro

Komal Sodhi, Sarah Stevens, Morghan Getty, Rebecca Hutcheson, Joseph I Shapiro, Department of Medicine and Surgery, Joan C. Edwards School of Medicine, Marshall University, Huntington, WV, 25755 USA

Paola Pesce, David Sacerdoti, Department of Medicine (DIMED), University of Padova, Padova, Italy

Paola Pesce, Nitin Puri, Department of Physiology and Pharmacology, University of Toledo, Ohio, USA

Gaia Favero, Rita Rezzani, Department of Clinical and Experimental Sciences, Division of Anatomy and Physiopathology, University of Brescia, Brescia, Italy

Correspondence to: Komal Sodhi, M.D, Assistant Professor of Surgery and Pharmacology, Marshall University Joan Edwards School of Medicine, WV 25701, USA

Email: Sodhi@marshall.edu

Telephone: +1-304-691-1700 Fax: +1-914-347-4956

Received: December 30, 2014 Revised: January 29, 2015

Accepted: February 3, 2015

Published online: April 10, 2015

ABSTRACT

BACKGROUND: Cardiovascular risk and therapy in immunodeficient patients is a challenge for cardiologists. T regulatory lymphocytes (Treg) are a subpopulation of T helper lymphocytes that plays an important role in post-ischemic cardiac remodeling. Nitric oxide (NO) plays a central role in vascular response to ischemic damage by decreasing microvascular resistance and is an important regulator of the immune system. The therapeutic effect of HO-1 induction during cardiac ischemic damage has been studied but its effect in immunosuppressed mice remains to be tested. The aim of this study was to assess the beneficial role of HO-1 upregulation in attenuating cardiac remodeling after onset of myocardial infarction (MI) in immuno-suppressed mice.

METHOD: Myocardial infarction was induced by LAD ligation in immunosuppressive (BALB SCID) mice. Mice comprised 4 groups: sham, MI, MI treated with the HO-1 inducer cobalt protoporphyrin (CoPP) with and without HO activity inhibitor, tin mesoporphyrin (SnMP).

RESULTS: Mice with MI had increased levels of inflammatory cytokines, myocardial fibrosis and myocyte death ($p<0.05$) as compared to control animals. Left ventricle end diastolic area (EDA) was reduced and fractional area change (FAC) and angiogenesis was increased ($p<0.01$) in CoPP-treated mice compared to the MI group. Inflammation, cardiac iNOS expression, myocardial cell death and fibrosis were reduced in CoPP treated animals as a result of increased bilirubin levels ($p<0.05$) serum nitrite levels were increased. Foxp3 (marker of T regulatory cells), pAMPK, pAKT expression in cardiac tissues was increased in CoPP-treated animals. SnMP reversed these positive cardiac effects.

CONCLUSION: This novel study suggests that Upregulation of HO-1 improves cardiac function and microvascular tone control after onset of MI in immuno-suppressed mice probably through an increase of NO bioavailability and bilirubin levels and a decrease in inflammatory cytokines.

Key words: Immunodeficiency; HO-1; NO; MI; Cardiac function; Neoangiogenesis

Sodhi K, Pesce P, Stevens S, Getty M, Puri N, Favero G, Rezzani R, Hutcheson R, Sacerdoti D, Shapiro JI. Upregulation of Heme Oxygenase-1 Attenuates Ischemic Heart Myocyte Cell Death and Improves Heart Function in Immunosuppressed Mice. *Journal of Cardiology and Therapy* 2015; 2(2): 291-301 Available from: URL: http://www.ghrnet.org/index.php/jct/article/view/972

Abbreviations

3:-T : 3-Nitrotyrosine
Akt: Serine/threonine Protein Kinase

AMPK: AMP-activated Protein Kinase
AWT: Anterior wall thickness
CoPP: Cobalt Protoporphyrin
CO: Carbon Monoxide
CAD: Coronary Artery Disease
EDA: End Diastolic Area
EDD: End Diastolic Diameter
ESA: End Systolic Area
ESD: End Systolic Diameter
EDV: End Diastolic Volume
ESV: End Systolic Volume
EF: Ejection Fraction
ET: Ejection Time
eNOS: Endothelial Nitric Oxide Synthase
FAC: Fractional Area Change
FAS: Fractional Area Shortening
Foxp3: Fordhead Box Protein P3
HO-1 : Heme Oxygenase Isozyme 1, inducible form
IL-6: Interleukin 6
iNOS: Inducible Nitric Oxide Synthase
IVCT: Isovolumetric Contraction Time
IVRT: Isovolumetric Relaxation Time
LAD: Left Anterior Descending
LV: Left Ventricle
MI: Myocardial Infarction
MPI: Myocardial Performance Index
NADPH: Nicotinamide Adenine Dinucleotide Phosphate (reduced form)
NO: Nitric Oxide
NOS: Nitric Oxide Synthase
peNOS: Phosphorylated Endothelial Nitric Oxide Synthase
PWT: Posterior Wall Thickness
ROS: Reactive Oxygen Species
SCID: Severe Combined Immunodeficiency
SnMP: Tin Mesoporphyrin IX Dichloride
Treg: T Regulatory Cells
TNF α: Tumor Necrosis Factor-Alpha
TXA2: Thromboxane A2

INTRODUCTION

Myocardial infarction (MI) is a life-threatening dynamic process initiating with coronary occlusion and frequently progressing towards chronic heart failure. Myocardial dysfunction and coronary macro/microvascular alterations are the hallmarks of cardiac failure and are ascribed to increased oxidative stress and altered nitric oxide synthase (NOS) activity[1]. Oxidative stress associated with deficient antioxidant systems has been reported to play a critical role in subcellular remodeling in patients with myocardial infarction. The heme-HO system, is one of the key defense mechanism against oxidative stress[2]. The effect of increased levels of HO-1 is attributable, in large part, to the degradation of heme from denatured heme protein to bilirubin/biliverdin, iron and carbon monoxide (CO)[3-6].

Bilirubin formation efficiently scavenges reactive oxygen species (ROS) and peroxyl radicals[7,8]. Bilirubin is a potent antioxidant and patients with Gilberts disease have elevated levels of bilirubin and do not develop cardiovascular disease[2,9]. Numerous reports indicate that a higher serum bilirubin is associated with a decrease in the risk for coronary artery disease, which was related to decrease in NADPH oxidase and enhancement of endothelial function[10-13]. HO-1-derived bilirubin has also been shown to display cytoprotective properties in the cardiovascular system. In animal models of myocardial ischemia, over expression and/or pharmacological induction of HO-1 improved cardiac function and promoted neoangiogenesis[14,15]. However, little is known about the potential beneficial effects of HO-1 in immuno-suppressed animal models of myocardial infarction. There is evidence that HO-1 plays an immuno-modulative role although the underlying molecular mechanism remains unclear. Accumulated evidence supports an immunoregulatory function for HO-1 e.g. HO-1 overexpression prevents graft rejection in organ transplantation by acting on the lymphocyte-mediated immune response[16-18]. These findings support the functional importance of HO-1 in immune regulation.

Immunodeficiency is related to an increased cardiovascular risk, especially in HIV infected individuals. Cardiovascular disease, and particularly coronary artery disease (CAD), is an emerging area of concern in the immune-suppressed population. A 50% increased risk for myocardial infarction (MI) has been observed in Western countries in HIV-infected patients as compared to the general population[19]. The pathophysiology of this accelerated atherosclerotic process is complex and multifactorial; numerous studies suggest a role of impaired immune response and chronic inflammation that leads to vascular dysfunction and atherothrombosis[20]. Lymphocyte mediated immune response together with inflammation and oxidative stress plays a central role in the pathogenesis of atherosclerotic plaque evolution and myocardial infarction[21]. Subjects with early clinical presentation of coronary artery disease are characterized by a lower T lymphocyte levels and an altered CD4/CD8 ratio[22]. The major decline in CD4 count is associated with a marked increased risk of cardiovascular disease and death among HIV patients[23]. The role of different lymphocyte subpopulations in myocardial remodeling remains unclear. B lymphocytes, after myocardial ischemia, produce autoantibodies which are detrimental and contribute to autoimmunity and chronic heart failure, but B cell isotype IgM preserve ventricular function after ischemia reperfusion damage[24]. A subtype of T cells, regulatory T (Treg) cells, plays an important role in controlling both the innate and adaptive immune responses under physiological and pathological conditions[25,26]. The suppressive function of Treg cells is mediated through direct interaction with target cells and/or secretion of soluble factors such as interleukin-6 (IL-6)[25]. Treg cells also serve to protect against adverse ventricular remodeling and to improve cardiac function after MI via inhibition of inflammation and direct protection of cardiomyocytes[25]. This has led to the hypothesis that immunomodulation of the T lymphocyte immune response could improve post-ischemic cardiac remodeling.

Nitric oxide (NO) signaling is involved in the genesis of myocardial and vascular damage and an altered expression of nitric oxide synthase (NOS) isoforms occurs in cardiovascular dysfunction[27-29]. Cao et al have reported that CoPP treatment improves both cardiac function and coronary flow in infarcted rats by blunting restoring eNOS/iNOS expression balance and increasing HO-1 levels[1]. Also NO is increasingly recognized as an important regulator of the immune system[30]. During immune responses, activated T cells, via cytokines and perhaps other factors, induce expression of iNOS in immunosuppressive cells[31,32]. NO or other reactive nitrogen species from iNOS in these cells inhibit proliferation of T cells. NO bioactivity from iNOS has also been shown to contribute to elimination of activated effector T cells in the contraction phase of immune responses, probably through increasing T cell apoptosis[33,34].

In the present study we hypothesize that the increased expression of HO-1 attenuates cardiac dysfunction at least in part, through a NO mediated effect and via increase in bilirubin levels in immunosuppressed mice. Our novel study demonstrates the beneficial role of HO-1 Upregulation following coronary occlusion to benefit infarcted and remote territories, administered 5 days after the onset of cardiac remodeling, leading to improved cardiac function in immunosuppressed mice.

MATERIALS AND METHODS

Animal treatment

All animal studies were approved by the University of Toledo Animal Care and Use Committee in accordance with the National Institutes of Health Guidelines for Care and Use of Laboratory Animals. 32 BALB SCID (animals have reduced levels of B and T cells and 32 BALBc WT male mice) weighing 22-26 g at an age of 8 to 10 weeks were purchased from Jackson laboratories[35]. BALB SCID mice carry a DNA repair defect in the rearrangement of genes that code for antigen-specific receptors on lymphocytes. SCID mice are characterized by an early in vivo destruction of T and B progenitors, absence of functional T and B cells, lymphopenia and hypogammaglobulinemia, but they have a normal hematopoietic microenvironment and normal antigen presenting cells. The hematopoietic microenvironment is responsible for "badly-rearranged" lymphocyte progenitor destruction. Some SCID mice spontaneously develop partial immune reactivity and active T cells may be detected in a small number of animals which are considered "leaky". SCID leakiness is highly strain dependent, increases with age, and is increased in mice housed under non-specific pathogen free conditions. In general, SCID leakiness is higher in animals with the BALB genetic background[35]. Mice were housed under SPF conditions in a single ventilated cage system, fed standard mouse chow and water ad libitum. SCID and WT mice were divided randomly into four groups: sham operated animals, MI mice and MI mice treated with an inducer of HO-1, CoPP, in the absence or presence of the HO activity inhibitor, SnMP. All MI animals underwent left anterior descending (LAD) artery ligation through the transthoracic approach. 5 days after surgery, CoPP was administered intraperitoneally every 5 days for three weeks at a concentration of 3 mg/kg body weight. SnMP was injected intraperitoneally, 3 times a week at a dose of 20 mg/kg of body weight, for 2 weeks. All animal groups underwent echocardiography examination 30 days after surgery and were sacrificed immediately. Euthanasia was accomplished with the delivery of 100% CO_2 via a compressed gas cylinder. Blood samples were collected in K3EDTA tubes at sacrifice and the plasma was separated. Samples were flash frozen in liquid nitrogen and maintained at -80℃ until assayed.

Left anterior descending coronary artery ligation (LAD)

Animals were anesthetized using ketamine and xylazine (80 mg/Kg and 10 mg/Kg respectively), chest shaved, endotracheal intubated and ventilated with 100% oxygen and isoflurane (0.75% to 1.5%) at 180 breaths per minute using a MiniVent Mouse Ventilator (type 845, Harvard Apparatus). A heating pad was used to maintain body temperature at 37℃. Under sterile conditions, a left thoracotomy was performed in the 3th intercostal space, the heart exposed and the pericardium opened. An 8.0 prolene ligature (Ethicon) was passed and tied around the proximal left coronary artery, just distal to the left atrial appendage border. Blanching of the anterolateral region of the left ventricle (LV) confirmed infarction. The chest was then closed with a single 5.0 silk suture between the 3th and 4th ribs, the muscle layers were recomposed and the skin closed with continuous suture. After surgery, all mice were hydrated with saline and given analgesic, carprofen at the dose of 4 mg/Kg subcutaneously, for two days. At the end of the surgery mice were housed for 24 hours in an incubator at 37℃ and then recovered in single cages and monitored twice a day for 7 days. Sham surgery was performed following the same procedure without coronary ligation.

Echocardiography

Transthoracic echocardiography was performed using a Siemens Acuson Sequoia echo machine with a 15 MHz linear probe. Animals had their chests shaved after being anesthetized with 3% isoflurane; temperature controlled anesthesia was maintained with 1.5% isoflurane. Two-dimensional cine loops and M-mode cine loops of a long-axis view and a short-axis view of the Left Ventricle (LV) were recorded. Anterior wall thickness (AWT), End Diastolic Diameter (EDD) and End Systolic Diameter (ESD) of LV, Posterior Wall Thickness (PWT), End Diastolic Area (EDA) and End Systolic Area (ESA) were measured from recorded cine-loop. M-mode cine loop of the aortic valve was recorded and Doppler analysis of LV flow was performed from the long axis B-mode image placing the sample volume in the LV, below the mitral annulus and Aortic Ejection Time (ET), Isovolumetric Contraction Time (IVCT) and Isovolumetric Relaxation Time (IVRT) were measured and Myocardial Performance Index (MPI) was calculated (MPI=IVCT+IVRT/ET). All mice were imaged by a single operator. Fractional Area Change (FAC) was determined with the formula: EDA-ESA/EDA. End diastolic volume (EDV), end systolic volumes (ESV) and ejection fraction (EF) were determined using the following simplified formulas: EDV= (3.14/6)*EDD*EDD*EDL, ESV=(3.14/6)*ESD*ESD*ESL and EF =(EDV-ESV)/EDV.

Histopathological analyses

Hearts were fixed in 4% paraformaldehyde and embedded in paraffin wax according to standard procedures and serial sections cut using a microtome (7 μm thickness). Embedded paraffin sections were deparafinized, rehydrated and finally stained with hematoxylin-eosin and Masson tricrome staining. In particular Masson tricrome staining showed collagen fibers in blue and cytoplasm in red. A minimum of 20 fields for each slide was examined and evaluated for the presence of necrosis and inflammatory infiltration by two observers blinded to the treatments.

Immunohistochemistry analyses for CD31

Embedded sections were deparafinized, rehydrated and subjected to antigen retrieval in 0.05 M sodium citrate buffer (pH 6.0) in a microwave oven. Endogenous peroxidase activity was blocked by incubation with a solution of 3% hydrogen peroxide in methanol for 30 minutes. The sections were then incubated with the appropriate normal serum (Vector Labs., Burlingame, CA, US) for 1 h and successively with rat monoclonal antibody against CD31 for 1 h at room temperature and overnight at 4℃. After incubation in primary antibody, the sections were sequentially incubated in the appropriate biotinylated immunoglobulins, avidin-biotin peroxidase complex (Vector Labs., Burlingame, CA, US) and in a solution of 0.05% 3-3-diaminobenzidine tetrahydrochloride (Sigma Aldrich, St. Louis, MO, US) and 0.33% hydrogen peroxide. All sections were finally counterstained with hematoxylin, dehydrated and mounted. Control reactions were performed by omitting the primary antibody and with isotype-matched irrelevant IgGs as the negative control.

Quantitative analyses

During quantitative analyses two observers blinded to the treatments computed blue staining for the Masson thricrome staining and immunopositivity for both immunohistochemistry and immunofluorescence. Digitally fixed images of the slices (×400 magnification) were analyzed using an image analyzer (Image Pro Plus, Milan, Italy). The blue staining and the immunopositivity were calculated for arbitrary areas, measuring 20 random fields with the same area for each sample. The data were pooled to represent a mean value and a statistical analysis was applied to compare the results obtained from the different experimental groups.

Western blot analysis of Cardiac tissue

Frozen Heart tissue was pulverized under liquid nitrogen and placed in a homogenization buffer comprising (mmol/L): 10 phosphate buffer, 250 sucrose, 1 EDTA, 0.1 PMSF and 0.1% v/v tergitol, pH 7.5. Homogenates were centrifuged at 10,000 g for 10 minutes at 4ºC. The supernatant was isolated and protein levels were assayed (Bradford Method). The supernatant was used for the determination of HO-1, 3NT, pAKT, AKT, pAMPK, AMPK, iNOS, Fox p3, CD3 and TXA2. Immunoblotting was performed in heart tissue as previously described[36,37]. β Actin was used to ensure adequate sample loading for all Western blots.

Cytokines measurements

The plasma levels of TNF-α, IL-6 were determined using an ELISA assay as previously described[36,38].

Serum Nitrite measurement

Serum nitrite was determined using an ELISA assay according to the manufacture's protocol (Sigma Aldrich). Briefly, a nitrite standard solution was serially diluted (200-1.6 mM) in duplicate in a 96-well, flat-bottomed polystyrene microtitre plate (Polylab). The diluting medium was used as standard blank. After loading the plate with samples (100 mL), addition of VCl3 (100 mL) to each well was rapidly followed by addition of the Griess reagents, sulfonamide (100 mL) and NED (100 mL). The absorbance at 540 nm was measured in a plate reader after incubation for 30 min in the dark.

Serum Bilirubin measurement

Bilirubin formation was determined, in an Aminco (Urbana, IL) DW-2C spectrophotometer, by using the difference in absorption from 460 to 530 mm. Blanks for the assay were prepared by adding $HgCl_2$ to a final concentration of 4mM in the complete assay mixture.

Statistical analysis

Data are expressed as mean±S.E.M. Significance of difference in mean values was determined using one-way analysis of variance followed by the Newman-Keul's post hoc test. $P<0.05$ was considered to be significant.

RESULTS

CoPP improves cardiac function in BALB SCID mice 30 days after MI

BALBc WT and SCID mice were comparable with regard to age, body weight and heart rate at the moment of initial echocardiographic analysis. No significant difference in left ventricle morphology and function was found on the basal echo. In the MI group 30 days after LAD ligation the End Diastolic Area (EDA) was increased as a consequence of the dilatation of the left ventricle due to the myocardial remodeling after ischemic damage (Figure 1 A, B and E; $p<0.05$) and Fractional Area Change (FAC) was reduced as consequence of the reduction of contractile function (Figure 1 F; $p<0.05$). Posterior wall thickness (PWT) was increased ($p<0.05$) as consequence of the reactive hypertrophy of the posterior wall. Moreover in the MI group the MPI, measured as an index of diastolic function, was reduced (Table 1; $p< 0.05$). After CoPP treatment the improvement of heart contractile function (FE, FAC) was significant as compared to MI group (Table 1, Figure 1 C and F; respectively $p<0.05$ and $p<0.01$). SnMP reversed the effect of CoPP on left ventricle dilatation and systolic function (Figure 1 D, E and F). The treatment with SnMP reversed the effect of CoPP on FAS and EDA levels ($p<0.05$). However, the dilatation of the left ventricle and the depression of heart function were more evident in SCID than in WT mice (S1 A and B). After treatment with CoPP the improvement of heart function was significant in both strain but more evident in SCID mice as if the immunosuppressive strain was more sensitive to the effect of HO-1 induction. The treatment with SnMP reversed the effect of CoPP on FAS and EDA in both strains; this effect of SnMP was more evident in SCID mice ($p<0.05$).

CoPP decreases Cardiac necrosis and fibrosis in BALB SCID mice 30 days after MI

In MI mice myocardial cell necrosis and lysis and inflammatory cells that had breached the myocardial cell death and necrotic area (Figure 2 A) were evident. CoPP-treated mice had a myocardial morphology comparable to control mice (Figure 2B, a and c); while SnMP-treated mice had a morphology similar to that of MI mice. (Figure 2B, b and d).

Histopathological examination of cardiac tissue (Figure 2B, a and b) revealed that collagen deposition was higher in hearts of MI mice as compared to the sham operated animals (Figure 2 a and b respectively; $p<0.05$). CoPP decreased myocardial cell death and fibrosis as compared with MI animals and the concurrent administration of SnMP increased cell death, collagen deposition to the levels of the MI mice (Figure 2B, c and d; $p<0.05$).

Table 1 SCID mice: in vivo heart measurements by echocardiography 30 days after LAD.

	SHAM (n=8)	MI (n=6)	MI+CoPP (n=6)	MI+CoPP+ SnMP (n=5)
Body weight (g)	27.4±2.8	27.8±2.2	26±1	25±0.8
Heart rate (bpm)	421±52	412±93	419±93	355±22
EDA (cm)	0.15±0.02	0.19±0.02**##	0.14±0.01§	0.17±0.01#
ESA (cm)	0.1±0.01	0.14±0.02**##	0.1±0.01§	0.12±0.01#
EDD (cm)	0.036±0.03	0.39±0.04**##	0.36±0.01§	0.39±0.03#
ESD (cm)	0.25±0.02	0.3±0.04**##	0.26±0.01	0.28±0.04
PWT (cm)	0.070±0.008§	0.08±0.01*#	0.064±0.01§	0.082±0.01*#
AWT (cm)	0.070±0.008§##	0.053±0.013**	0.048±0.005**	0.051±0.005*
FAC	0.34±0.04§	0.24±0.04**##	0.34±0.03§§	0.27±0.01**##
EF	0.60±0.06§	0.46±0.1**#	0.57±0.06	0.52±0.04 *
ET (msec)	59.2±6.5§	59.6±6.3§	55±6§§	66.7±4.7
IVCT+IVRT (msec)	17.4±4.2§§	27.6±12.7*	19.6±4.8§	26.5±2.3
MPI	0.29±0.08§	0.47±0.2*	0.35±0.09	0.40±0.05

Values are expressed as mean±SD; n=number of animals tested; $p<0.05$ and **$p<0.01$ vs sham; #$p<0.05$ and ##$p< 0.01$ *vs* CoPP-treated group; §$p<0.05$ and §§$p<0.01$ *vs* CoPP+SnMP group.

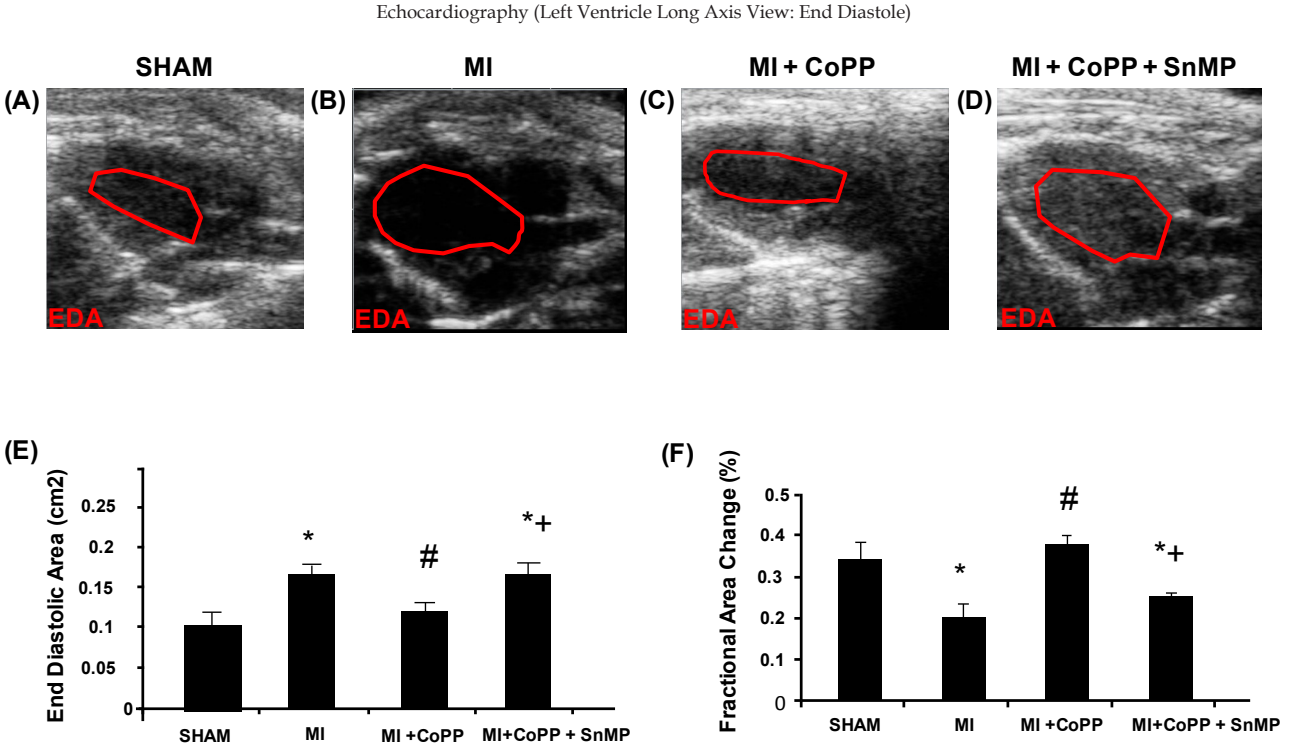

Figure 1 Effect of CoPP on Fractional Area Shortening and End Diastolic Area measured by Echocardiography in SCID mice 30 days post MI; Results are expressed as the mean±SE, *n*=6/ group. (A, B, C, D) echocardiographic images of LV long axis view and EDA trace (E) End Diastolic Area (CM^2) of SCID mice, **p*<0.05 *vs* Sham, #*p*<0.05 *vs* MI, +*p*<0.05 *vs* MI+CoPP (F) Fractional Area Shortening (%) of SCID mice, **p*<0.05 *vs* Sham, #*p*<0.05 *vs* MI, +*p*<0.05 *vs* MI+CoPP.

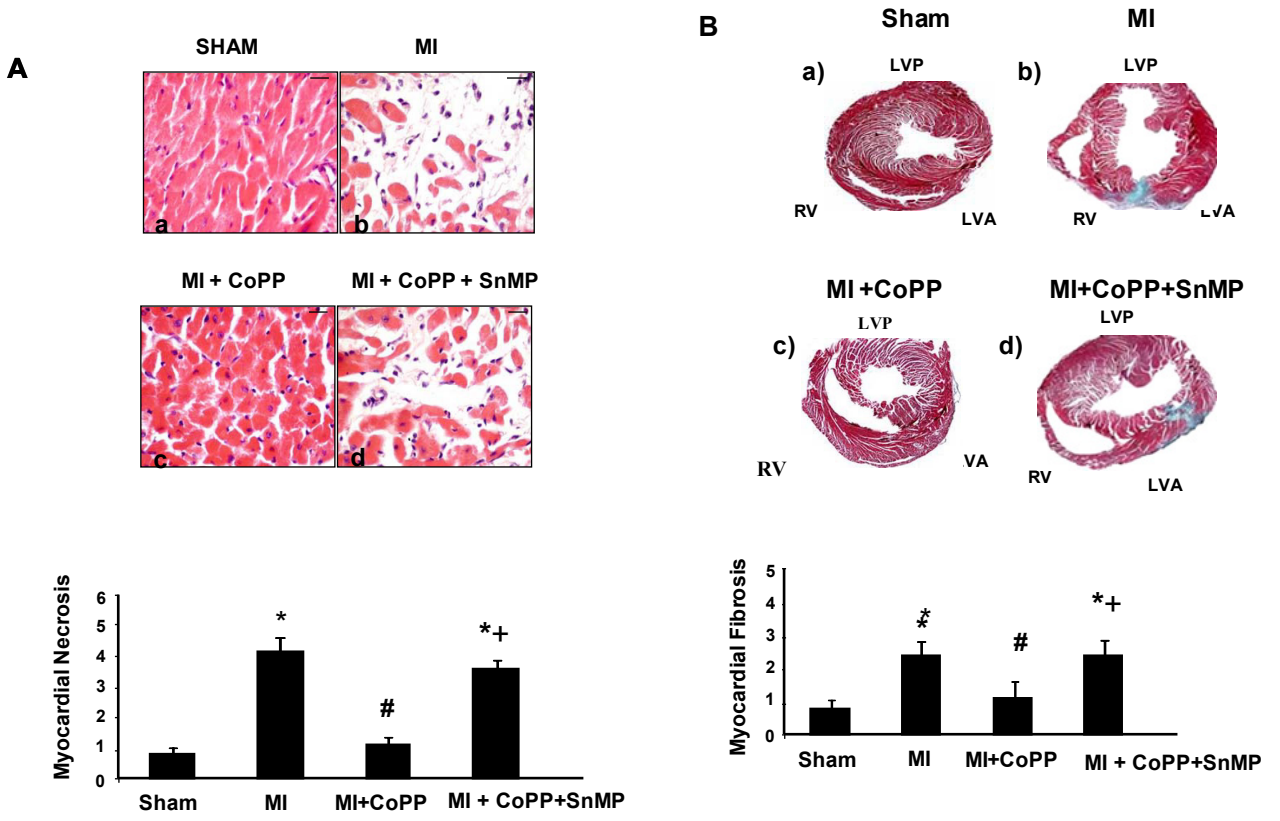

Figure 2 (A) Effect of CoPP on Cardiac Necrosis in SCID mice 30 days post MI. Hematoxylin-eosin staining was used to evaluate necrosis. (b,d) Necrotic myocytes are characterized by loss of cellular membrane (cellular lysis) **p*<0.05 *vs* Sham, #*p*<0.05 *vs* MI, +*p*<0.05 *vs* MI+CoPP. (B) Effect of CoPP on Cardiac Fibrosis in SCID mice 30 days post MI. Results are expressed as the mean±SE, *n*=6/ group. (a, b, c, d) Masson trichrome staining for Myocardial Fibrosis in SCID mice; (e)**p*<0.05 *vs* Sham, #*p*<0.05 *vs* MI, +*p*<0.05 *vs* MI+CoPP.

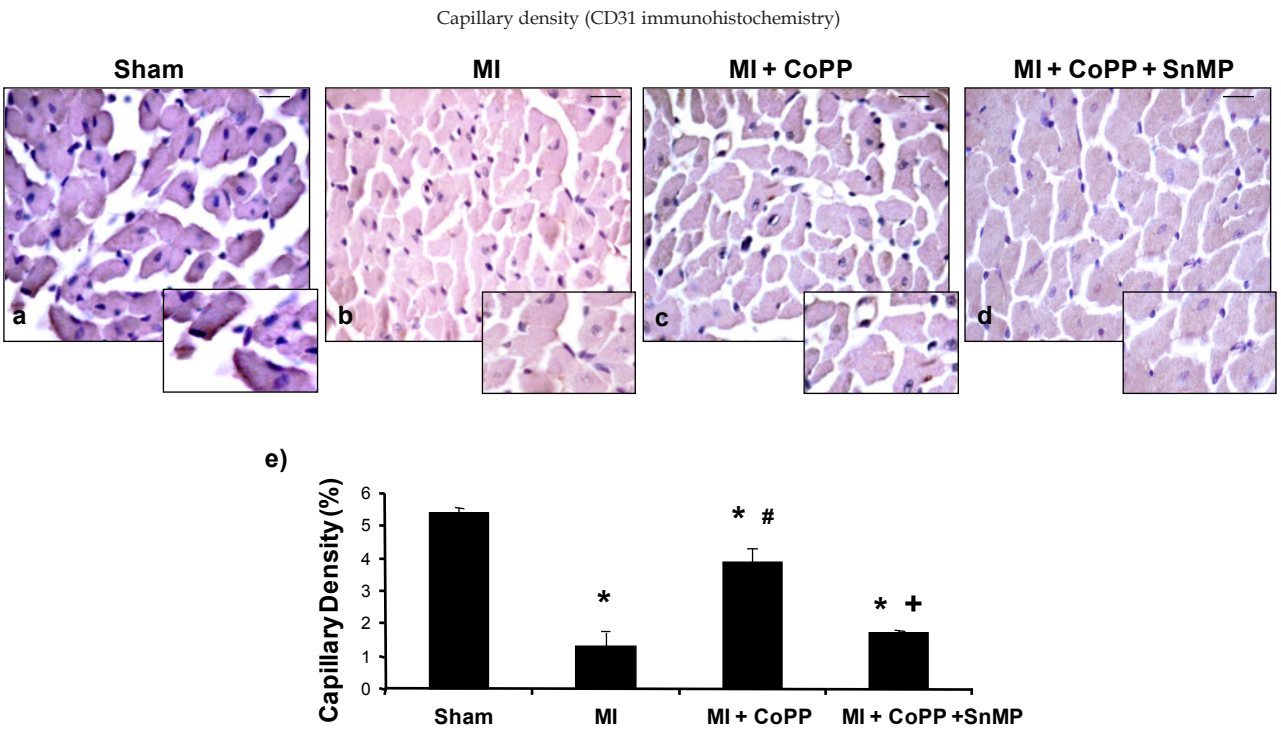

Figure 3 Immunohistochemistry images of CD31 expression of heart in SCID mice. The graph shows the histomorphometrical analyses of CD31 immunopositivity in mice heart samples. *p<0.05 *vs* sham; #p<0.05 *vs* MI, +p<0.05 *vs* MI+CoPP.

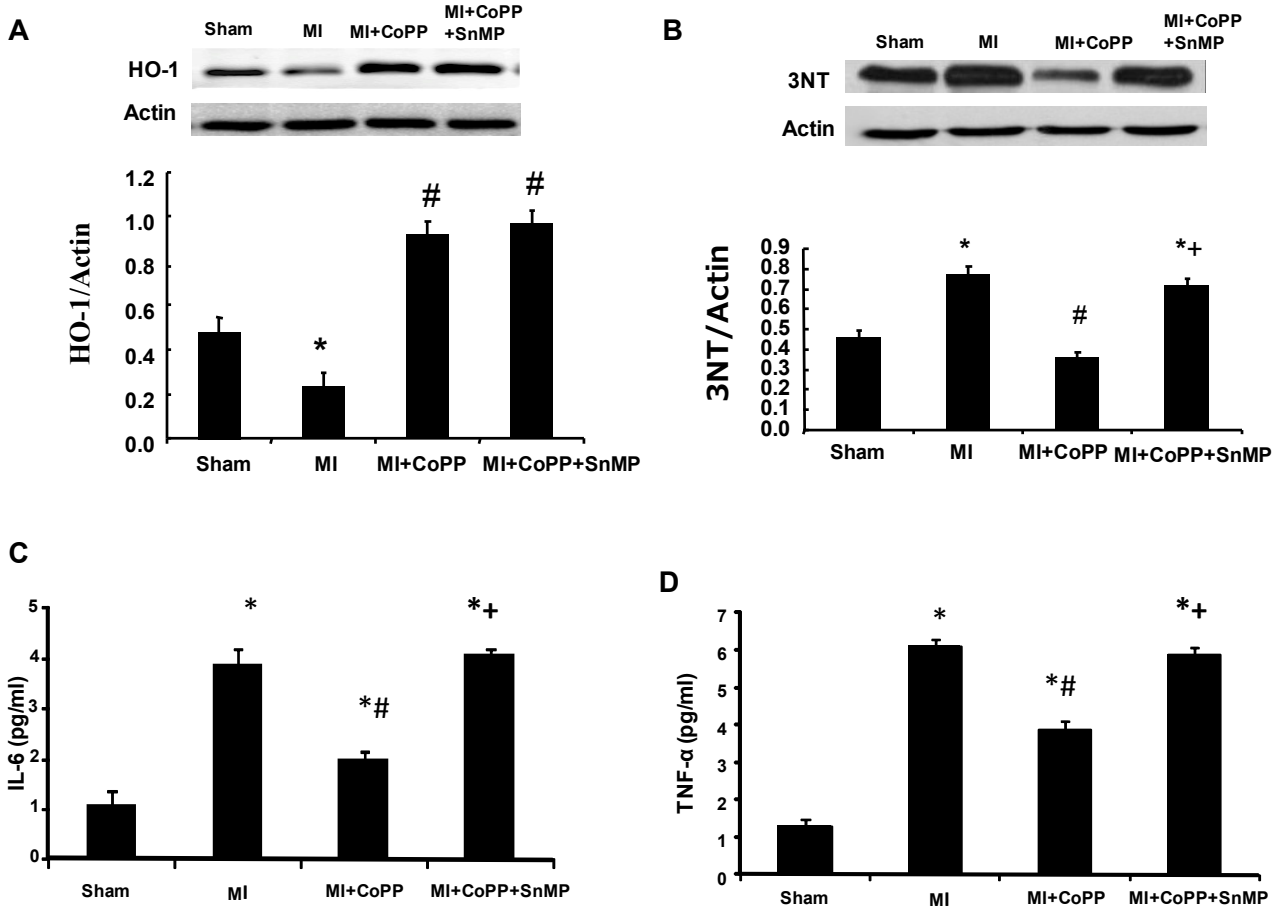

Figure 4 (A,B) Effect of CoPP on the expression of HO-1 and 3NT in heart tissue in SCID mice 30 days post MI. Data are shown as mean band density normalized to β-actin. Results are expressed as the mean±SE, n=6/group. Western blot and densitometry analysis of HO-1 and 3NT expression in SCID mice. (C,D) Effect of CoPP on plasma Cytokines in SCID mice 30 days post MI. (C) Plasma IL-6 level of SCID mice; *p<0.05 *vs* Sham, #p<0.05 *vs* MI, +p<0.05 *vs* MI+CoPP; (D) Plasma TNF alpha level of SCID mice; *p<0.05 *vs* Sham, #p<0.05 *vs* MI, +p<0.05 *vs* MI+CoPP.

CoPP increases Capillary density in BALB SCID mice 30 days after MI

CD31 immunohistochemistry of cardiac tissue revealed a reduction in capillary density in the hearts of MI mice as compared to the sham operated animals (Figure 3 A and B; $p<0.05$). CoPP increased the capillary density as compared to MI mice while SnMP reduced the beneficial effects of CoPP treatment to levels similar to those found in the MI mice (Figure 3 C and D; $p< 0.05$).

Effect of CoPP on HO-1 and 3NT expression in BALB SCID mice 30 days after MI

Western blot analysis of HO-1 in cardiac tissue, normalized against actin, showed a decrease in HO-1 expression in the SCID MI group. CoPP increased HO-1 expression in SCID mice (Figure 4A; $p<0.05$). In addition, SnMP also increased HO-1 expression confirming previous results. These findings are not surprising as SnMP, which induced a significant increase in HO-1 expression, is a potent inhibitor of HO activity, as shown previously[4,39,40] and thus prevents heme degradation and inhibits formation of HO products i.e. CO and bilirubin. Further our results showed that in WT mice the increase in HO-1 expression was less than SCID mice after treatment with CoPP (S2) suggesting that the immunosuppressive strain was more sensitive to the effect of HO-1 induction. 3NT, a marker of oxidative stress, was increased in the SCID MI group when compared to the sham group. CoPP reduced cardiac expression of 3NT (Figure 4B; $p<0.05$). The concurrent administration of SnMP increased the expression of 3NT to levels comparable to MI mice ($p<0.05$).

CoPP decreases plasma inflammatory cytokines in BALB SCID mice 30 days after MI

Systemic inflammation was examined by the measurement of circulating inflammatory markers IL-6 and TNFα. Plasma IL-6 (Figure 4C) and TNFα (Figure 4D) were both increased in MI mice as compared to the sham group ($p<0.05$). The administration of CoPP 5 days after the MI decreased inflammation and this effect was reversed by SnMP ($p<0.05$). Further, our results showed that SCID mice have an increased basal production of cytokines despite a decreased lymphocyte expression as compared to WT mice (S3 B and C). After treatment with CoPP the decrease in IL-6 was 51% in SCID mice with MI as compared to WT mice (33% decrease with CoPP treatment; Figure 5C). Similarly after CoPP treatment in SCID mice with MI, the levels of TNFα was decreased by 34% (Figure 5D) as compared to 21% decrease in WT mice with MI and treated with CoPP (Figure S3; $p<0.05$); suggesting the immunosuppressive strain was more sensitive to the effect of HO-1 induction as compared to the WT mice. The treatment with SnMP reversed the effect of CoPP on cytokines level in both strains; this effect of SnMP was more evident in SCID mice ($p<0.05$); further suggesting that the beneficial role of HO-1 induction on SCID mice is probably due to an increase in Treg cells and decrease in cytokines levels.

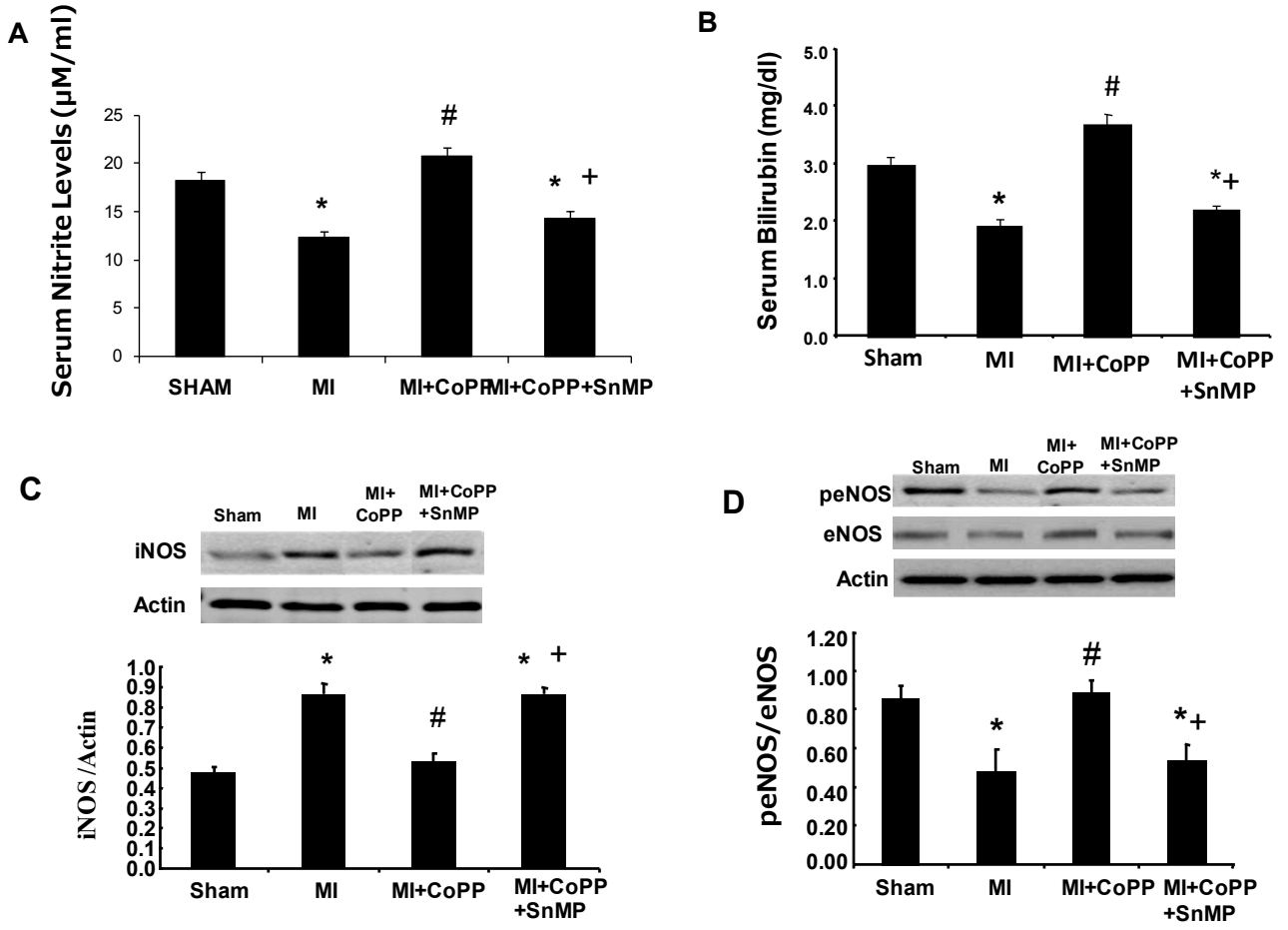

Figure 5 (A) Effect of CoPP on serum nitrite levels in SCID mice 30 days post MI, *$p<0.05$ *vs* Sham, #$p<0.05$ *vs* MI, +$p<0.05$ vs. MI+CoPP. (B) Effect of CoPP on serum bilirubin level in SCID mice 30 days post MI, *$p<0.05$ *vs* Sham, #$p<0.05$ vs. MI, +$p<0.05$ *vs* MI+CoPP. (C) Effect of CoPP on iNOS expression in heart tissue by western blot analysis in SCID mice 30 days post MI. (D) Effect of CoPP on peNOS/eNOS expression in heart tissue by western blot analysis in SCID mice 30 days post MI. Data are shown as mean band density normalized to β-actin. Results are expressed as the mean±SE, $n=6$/group. *$p<0.05$ *vs* MI; # $p<0.05$ *vs* MI+CoPP.

Effect of CoPP on serum nitrite, serum bilirubin and cardiac iNOS, peNOS expression in BALB SCID mice 30 days after MI

Serum nitrite used as an indicator of NO production, (Figure 5A) was decreased in SCID MI mice as compared to the sham group ($p<0.05$). The administration of CoPP 5 days after the MI increased serum nitrite levels, and this beneficial effect of CoPP was reversed by administration of SnMP ($p<0.05$). We measured serum bilirubin levels, a byproduct of heme degradation by HO-1, and our results showed that bilirubin levels followed the similar pattern as HO-1 expression. Serum bilirubin level was decreased in MI group as compared to the sham group (Figure 5B). CoPP increased the bilirubin level as compared to MI mice while SnMP reduced the beneficial effects of CoPP treatment to levels similar to those found in the MI mice ($p<0.05$; Figure 5B). Further our results showed that Cardiac iNOS was increased ($p<0.05$) in the MI group when compared to the sham group. CoPP reduced significantly cardiac expression of iNOS (Figure 5C). SnMP increased the expression of iNOS ($p<0.05$). In concordance with our hypothesis, cardiac tissue showed a decrease in the peNOS/eNOS ratio (Figure 5D; $p<0.05$) in the MI group as compared to the sham group. CoPP ($p<0.05$) increased peNOS expression and SnMP reversed this beneficial effect of CoPP. Therefore our results showed that CoPP increased NO bioavailability, restoring the balance of cardiac eNOS and iNOS isoforms and the redox state.

Effect of CoPP on pAMPK, pAKT and TxA2 expression in BALB SCID mice 30 days after MI

Western blot analysis of cardiac tissue showed a decrease in the pAMPK/AMPK and pAKT/AKT ratios (Figure 6 A and B respectively; $p<0.05$) in the MI group as compared to the sham group. CoPP ($p<0.05$) increased the phosphorylated form of both pAMPK and pAKT and this effect was reversed by SnMP. Cardiac TXA2, a marker of local inflammation, was increased ($p<0.05$) in the MI group when compared to the sham group. CoPP reduced cardiac expression of TXA2 (Figure 6C; $p<0.05$). SnMP increased the expression of TXA2 ($p<0.05$). Further, our results showed that SCID mice have an increased basal expression of TXA2 as compared to the WT mice (Figure 6C and S3 A respectively). After treatment with CoPP the decrease in TXA2 was 2 fold in SCID mice with MI as compared to WT mice (1.1 fold decrease with CoPP treatment; Figure 6C and S3 A respectively); suggesting the immunosuppressive strain was more sensitive to the effect of HO-1 induction as compared to the WT mice.

CoPP increases T regulatory cells in BALB SCID mice 30 days after MI

Fordhead box protein P3 (FoxP3) is a key marker for CD4+ regulatory T cells and was used to identify T reg cells by western blot analysis. There was no difference between the sham and MI groups. T reg lymphocytes were increased in CoPP treated mice compared to sham and MI groups while SnMP treatment reversed the CoPP effect (Figure 7; $p<0.05$).

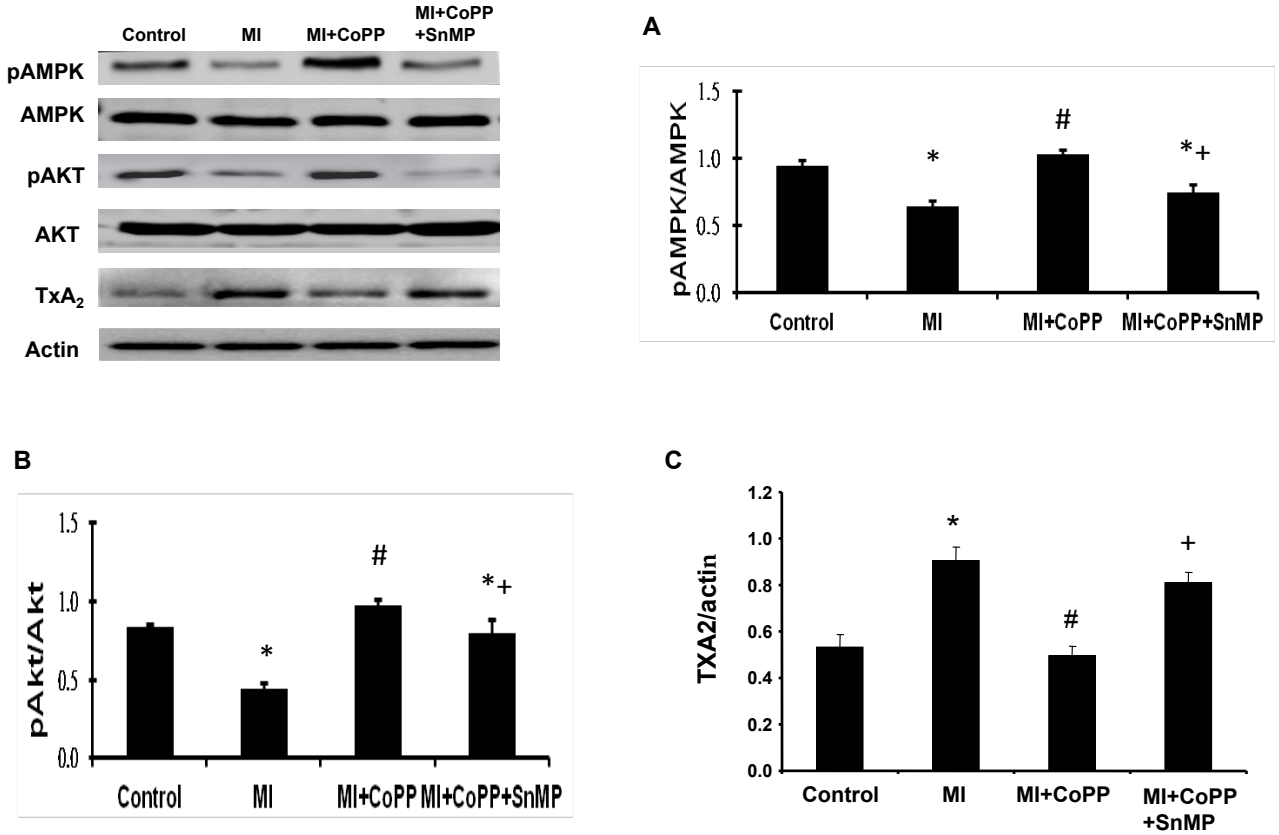

Figure 6 Effect of CoPP on the expression of pAMPK, pAKT and TXA2 Synthase in heart tissue in SCID mice 30 days post MI. Data are shown as mean band density normalized to β-actin. Results are expressed as the mean±SE, n=6/group; (A) Western blot and densitometry analysis of pAMPK expression in SCID mice respectively. (B) Western blot and densitometry analysis of pAKT expression in SCID mice respectively. (C) Western blot and densitometry analysis of TXA2 Synthase expression in SCID mice respectively. *$p<0.05$ *vs* Sham, #$p<0.05$ *vs* MI, +$p<0.05$ *vs* MI+CoPP.

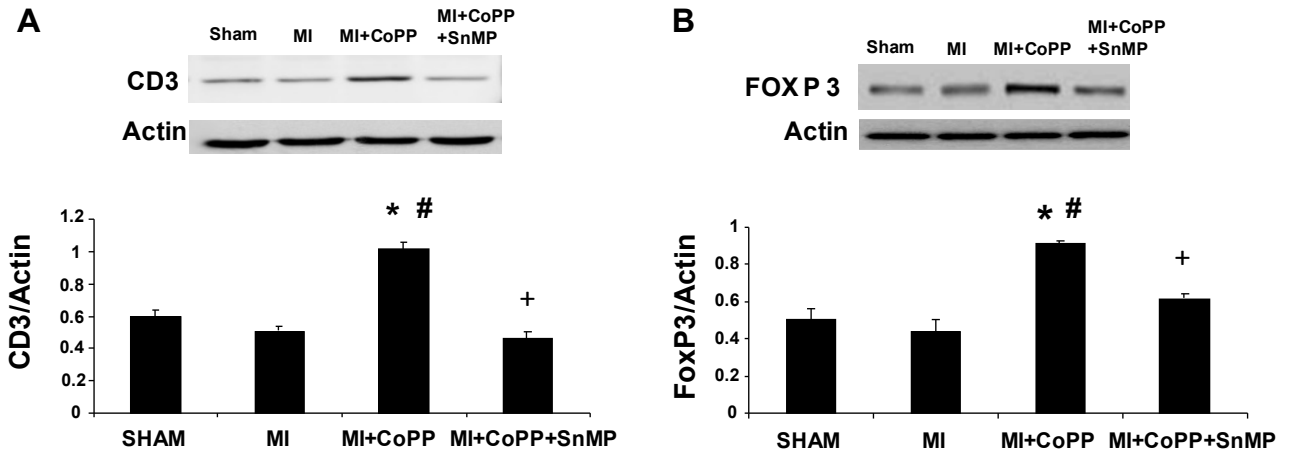

Figure 7 (A,B) Effect of CoPP on CD3 and FOXP3 expression in heart tissue by western blot analysis in SCID mice 30 days post MI. Data are shown as mean band density normalized to β-actin. Results are expressed as the mean±SE, n=6/group. *p<0.05 *vs* MI; #p<0.05 *vs* MI+CoPP.

DISCUSSION

This is the first study demonstrating the complete reversal of LV systolic dysfunction 5 days after the onset of cardiac remodeling in immuno-suppressed mice. HO-1 induction improved both cardiac function and coronary flow by blunting oxidative stress, restoring eNOS/iNOS expression balance and increasing bilirubin levels, thereby favoring improvement in cardiac function in immunosuppressed mice with post infarcted myocardium. Our results demonstrate that up regulation of HO-1 alleviates post infarction pathological LV remodeling, an effect mediated at least in part by bilirubin, by increasing Treg cells, restoring NO bioavailability, improving neo-angiogenesis and decreasing cell death and fibrosis and inflammatory cytokines.

Cardiac function, when examined by echocardiography, demonstrated detrimental alterations in LV morphology, systolic and diastolic function in the MI group as compared to the sham operated mice. Histological analysis confirmed the echocardiographic findings demonstrating necrotic myocytes in the hearts of the MI group (Figure 2B). Necrotic and apoptotic myocytes release ROS[14,41,42]. In conditions of oxidative stress, NO contributes to the formation of RNS, including peroxynitrite that exert cytotoxic actions in myocardial tissue[43]. In agreement with these observations we show, a significant increase in 3NT in the hearts of the MI group. Previous reports have shown that cytokines induce expression of iNOS in immunosuppressive cells[31,32]. NO bioactivity from iNOS has been shown to contribute to elimination of activated effector T cells, probably through increasing T cell apoptosis[33,34] further worsening the lymphocyte immunosuppressive condition of BALB SCID mice. In the present study the increased production of inflammatory cytokines in MI group was associated with an increased expression of iNOS. We also show a reduction in serum nitrite levels in mice with MI; suggesting a decreased NO availability during myocardial infarction.

Cardiac myocyte cell death and fibrosis was increased in the MI group as compared to the sham group (Figure 2). The fibrotic area exhibits a reduced vascularization as demonstrated by a reduction in CD31 (PECAM-1) staining. During ischemic damage cardiac fibroblasts are activated by the local release of ROS by the necrotic cells and inflammatory cytokines[44,45]. ROS activated dendritic cells also produce TXA2 and its production is related to T-lymphocyte immunosuppression[46,47]. In our study cardiac TXA2 production was increased in the hearts of the SCID MI group, as if the lack of immune cells was counterbalanced by an increased local production of pro-inflammatory cytokines, thereby demonstrating a probable relationship between TXA2 production and lymphocyte immunosuppression. Inflammatory and fibrotic processes lead, not only, to a structural, but also, to a functional alteration of the LV[48,49]. Our echocardiographic findings demonstrate a loss of contractile function (Figure 1F, Table 1) and LV diastolic dysfunction in the MI group as compared to the sham group. In this mouse model of MI, LV diastolic dysfunction is probably due to the fibrosis of the ischemic area combined with hypertrophy of the non-ischemic wall (posterior wall). Our data demonstrate that, even when lymphocyte mediated immunity is suppressed in SCID mice; the local and systemic inflammation patterns are activated and are, in all probability, responsible for the pathological cardiac remodeling process.

Another key finding of the present study is the beneficial effect of HO-1 induction, at least in part, due to increase in bilirubin levels on post ischemic cardiac remodeling in immunosuppressive mice. The early inflammatory state of MI BALB SCID mice is the target of the HO-1 induction effect on post-ischemic cardiac pathological remodeling[50] as demonstrated by the reduction of IL-6, TNF alpha and TXA2 levels in the CoPP treated group. This beneficial effect of HO-1 on redox balance is likely driven by bilirubin, which efficiently scavenges ROS and peroxyl radicals[8,11,51]. In CoPP- treated mice the increased levels of bilirubin were associated with increases in AKT and AMPK phosphorylation (Figure 6). This increase in protein expression leads to increased cellular resistance against ischemic damage. This positive effect of HO-1 induction also reduced myocardial necrosis in the ischemic area (Figure 2). Moreover CoPP related reduced expression of i-NOS and increased levels of peNOS with a consequent increased NO availability improved coronary perfusion and thus attenuated necrotic and fibrotic area (Figure 2 A, B). CoPP-treated mice also displayed an increased angiogenesis as shown by an increase in CD31 staining. TXA2 negatively influences circulatory flow and predisposes the individual to thrombotic complications and thus inhibits neoangiogenesis[52]. Our study showed that reduced TXA2 production in CoPP-treated mice was associated with an increased capillary/myocyte ratio as shown by CD31 staining indicative of increased local neoangiogenesis. Echocardiographic evaluation confirmed a functional improvement in LV systolic function. SnMP reversed the molecular, histological

and morphological effects of CoPP confirming the beneficial role of HO-1 expression.

Another key finding is an increased expression of Treg cells in CoPP treated mice. T regulatory lymphocyte (Treg) plays an important role in post-ischemic cardiac remodeling. MI is considered an immunological stimulus because necrotic cells release proteins that are recognized as antigens and thus stimulate the immune response[53], lymphocyte activation and proliferation and antibody production. The expression of iNOS is known to be involved in T-lymphocytes apoptosis. As shown by our data HO-1 (Figure 7B) overexpression is related to a decreased expression of iNOS, thus to a supposed reduced apoptosis of lymphocytes progenitors. Among lymphocyte subpopulations, T regulatory (T reg) cells are a subfamily of T helper lymphocytes with an immunomodulative effect on other lymphocytes: T reg cells produce cytokines responsible for both inflammatory response lowering and the attenuation of ventricular remodeling post MI by reducing the phagocytic and fibrotic response[25]. T reg cells improve cardiac function after MI via inhibition of inflammation and direct protection of cardiomyocytes[54]. We observed that SCID mice have an increased production of cytokines despite a decreased lymphocyte expression. Thus we demonstrate that in lymphocyte deficient mice there is compensatory increased production of cytokines by antigen presenting cells despite a reduced presence of lymphocytes and this could be responsible of the increased cardiovascular mortality in immunodeficient patients. The beneficial role of HO-1 mediated increased bilirubin production on SCID mice is probably due to its effect on cytokines production and on T-lymphocytes progenitor reduced apoptosis through its iNOS mediated effect. It is known that Treg cells decrease inflammatory response and cytokines production thus we demonstrate that HO-1 immunomodulative effect increases Treg cells via i-NOS down-regulation, and reduce cytokines production that is responsible of cardiac damage after ischemia. T reg lymphocytes are involved in collagen deposition and fibrosis; in particular, an increase in T reg cells reduces fibrosis and improves neovascularization and recovery of viable myocardium. Our data demonstrate that CoPP administration increases T reg lymphocyte expression in SCID mice and this effect is reversed by the concurrent administration of SnMP (Figure 7). We show that HO-1 induction stimulates and modulates lymphocyte maturation through i-NOS down regulation, promoting T reg differentiation. We propose that an iNOS related reduction in lymphocytes precursor destruction together with the concurrent modulation of hematopoietic microenvironment derived cytokines promote the differentiation of lymphocytes into Tregs.

In summary, the results of this novel study demonstrate the pivotal role of pharmacological induction of HO-1, 5 days after onset of cardiac remodeling to benefit infarcted and remote territories, leading to better cardiac function in a 4-week MI outcome in immunosuppressed mice, at least in part, via increase in bilirubin levels and NO bioavailability. The ability to up-regulate HO-1 and improve post infarction cardiac function via its effect on nitrite synthesis offers a new clinical approach in the treatment of immunosuppressed patients with MI. This is an area of potential therapeutic targeting that needs to be further explored in immunosuppressed populations of Diabetes, organ transplantation, auto inflammatory diseases as well as autoimmune diseases.

ACKNOWLEDGMENTS

The authors wish to thank Dr. Stephen J. Peterson and Dr. Robert Touchon for their scientific input in the preparation of this manuscript. The authors wish to thank Ms. Jennifer Brown for her assistance in the preparation of this manuscript.

CONFLICT OF INTERESTS

There are no conflicts of interest with regard to the present study.

REFERENCES

1. Cao J et al: Cobalt-Protoporphyrin Improves Heart Function by Blunting Oxidative Stress and Restoring NO Synthase Equilibrium in an Animal Model of Experimental Diabetes. Front Physiol. 2012;3:160
2. Abraham NG, Kappas A: Pharmacological and clinical aspects of heme oxygenase. Pharmacol Rev. 2008;60:79-127
3. Cao J et al: Heme oxygenase gene targeting to adipocytes attenuates adiposity and vascular dysfunction in mice fed a high-fat diet. Hypertension. 2012;60:467-475
4. Sodhi K et al: EET agonist prevents adiposity and vascular dysfunction in rats fed a high fat diet via a decrease in Bach 1 and an increase in HO-1 levels. Prost Other Lipid Mediat. 2012;98:133-142
5. Vanella L et al: Crosstalk between EET and HO-1 downregulates Bach1 and adipogenic marker expression in mesenchymal stem cell derived adipocytes. Prostaglandins Other Lipid Mediat. 2011;96:54-62
6. Burgess A et al: Adipocyte heme oxygenase-1 induction attenuates metabolic syndrome in both male and female obese mice. Hypertension. 2010;56:1124-1130
7. Clark JE, Foresti R, Green CJ, Motterlini R: Dynamics of haem oxygenase-1 expression and bilirubin production in cellular protection against oxidative stress. Biochem J. 2000;348 Pt 3:615-619
8. Kaur H et al: Interaction of bilirubin and biliverdin with reactive nitrogen species. FEBS Lett. 2003;543:113-119
9. Vitek L et al: Gilbert syndrome and ischemic heart disease: a protective effect of elevated bilirubin levels. Atherosclerosis. 2002;160:449-456
10. Kwak JY, Takeshige K, Cheung BS, Minakami S: Bilirubin inhibits the activation of superoxide-producing NADPH oxidase in a neutrophil cell-free system. Biochim Biophys Acta. 1991;1076:369-373
11. Hopkins PN et al: Higher serum bilirubin is associated with decreased risk for early familial coronary artery disease. Arterioscler Thromb Vasc Biol. 1996;16:250-255
12. Kawamura K et al: Bilirubin from heme oxygenase-1 attenuates vascular endothelial activation and dysfunction. Arterioscler Thromb Vasc Biol. 2005;25:155-160
13. Mancuso C, Bonsignore A, Di SE, Mordente A, Motterlini R: Bilirubin and S-nitrosothiols interaction: evidence for a possible role of bilirubin as a scavenger of nitric oxide. Biochem Pharmacol. 2003;66:2355-2363
14. Buja LM: Myocardial ischemia and reperfusion injury. Cardiovasc Pathol. 2005;14:170-175
15. Cao J et al: High fat diet enhances cardiac abnormalities in SHR rats: Protective role of heme oxygenase-adiponectin axis. Diabetol Metab Syndr. 2011;3:37
16. Cheng C et al: Dendritic cell function in transplantation arteriosclerosis is regulated by heme oxygenase 1. Circ Res. 2010;106:1656-1666
17. Woo J, Iyer S, Mori N, Buelow R: Alleviation of graft-versus-host disease after conditioning with cobalt- protoporphyrin, an inducer of heme oxygenase-1. Transplantation. 2000;69:623-633
18. Gerbitz A et al: Induction of heme oxygenase-1 before conditioning results in improved survival and reduced graft-versus-host disease after experimental allogeneic bone marrow transplantation. Biol Blood Marrow Transplant. 2004;10:461-472

19. Boccara F et al: HIV and coronary heart disease: time for a better understanding. J Am Coll Cardiol. 2013;61:511-523
20. Freiberg MS et al: HIV infection and the risk of acute myocardial infarction. JAMA Intern Med. 2013;173:614-622
21. Robertson AK, Hansson GK: T cells in atherogenesis: for better or for worse? Arterioscler Thromb Vasc Biol. 2006;26:2421-2432
22. Brunetti ND et al: Lymphocyte subset characterization in patients with early clinical presentation of coronary heart disease. J Thromb Thrombolysis. 2012;34:475-482
23. Helleberg M et al: CD4 Decline Is Associated With Increased Risk of Cardiovascular Disease, Cancer, and Death in Virally Suppressed Patients With HIV. Clin Infect Dis. 2013;57:314-321
24. Marchant DJ et al: Inflammation in myocardial diseases. Circ Res. 2012;110:126-144
25. Tang TT et al: Regulatory T cells ameliorate cardiac remodeling after myocardial infarction. Basic Res Cardiol. 2012;107:232
26. Tang TT et al: Defective circulating CD4CD25+Foxp3+CD127(low) regulatory T-cells in patients with chronic heart failure. Cell Physiol Biochem. 2010;25:451-458
27. Ceriello A et al: Acute hyperglycemia induces nitrotyrosine formation and apoptosis in perfused heart from rat. Diabetes. 2002;51:1076-1082
28. Nagareddy PR, Xia Z, McNeill JH, MacLeod KM: Increased expression of iNOS is associated with endothelial dysfunction and impaired pressor responsiveness in streptozotocin-induced diabetes. Am J Physiol Heart Circ Physiol. 2005;289:H2144-H2152
29. Csont T et al: The involvement of superoxide and iNOS-derived NO in cardiac dysfunction induced by pro-inflammatory cytokines. J Mol Cell Cardiol. 2005;39:833-840
30. Bogdan C: Nitric oxide and the immune response. Nat Immunol. 2001;2:907-916
31. Albina JE, Abate JA, Henry WL, Jr.: Nitric oxide production is required for murine resident peritoneal macrophages to suppress mitogen-stimulated T cell proliferation. Role of IFN-gamma in the induction of the nitric oxide-synthesizing pathway. J Immunol. 1991;147:144-148
32. Mills CD: Molecular basis of "suppressor" macrophages. Arginine metabolism via the nitric oxide synthetase pathway. J Immunol. 1991;146:2719-2723
33. Dalton DK, Haynes L, Chu CQ, Swain SL, Wittmer S: Interferon gamma eliminates responding CD4 T cells during mycobacterial infection by inducing apoptosis of activated CD4 T cells. J Exp Med. 2000;192:117-122
34. Vig M et al: Inducible nitric oxide synthase in T cells regulates T cell death and immune memory. J Clin Invest. 2004;113:1734-1742
35. EP Les Senior Staff Scientist: A brief history of the two substrains of BALB/c, BALB/cJ, and BALB/cByJ available from animals resources. JAX NOTES. 1990;Issue 443, Fall
36. Sodhi K et al: Epoxyeicosatrienoic acid agonist rescues the metabolic syndrome phenotype of HO-2-null mice. J Pharmacol Exp Ther. 2009;331:906-916
37. Li M et al: Treatment of obese diabetic mice with a heme oxygenase inducer reduces visceral and subcutaneous adiposity, increases adiponectin levels, and improves insulin sensitivity and glucose tolerance. Diabetes. 2008;57:1526-1535
38. Kim DH et al: Heme oxygenase-mediated increases in adiponectin decrease fat content and inflammatory cytokines, tumor necrosis factor-alpha and interleukin-6 in Zucker rats and reduce adipogenesis in human mesenchymal stem cells. J Pharmacol Exp Ther. 2008;325:833-840
39. Sardana MK, Kappas A: Dual control mechanism for heme oxygenase: tin(IV)-protoporphyrin potently inhibits enzyme activity while markedly increasing content of enzyme protein in liver. Proc Natl Acad Sci U S A. 1987;84:2464-2468
40. Botros FT, Schwartzman ML, Stier CT, Jr., Goodman AI, Abraham NG: Increase in heme oxygenase-1 levels ameliorates renovascular hypertension. Kidney Int. 2005;68:2745-2755
41. Sovari AA, Shroff A, Kocheril AG: Postinfarct cardiac remodeling and the substrate for sudden cardiac death: role of oxidative stress and myocardial fibrosis. Expert Rev Cardiovasc Ther. 2012;10:267-270
42. Sun Y: Oxidative stress and cardiac repair/remodeling following infarction. Am J Med Sci. 2007;334:197-205
43. Weinstein SL et al: Phosphatidylinositol 3-kinase and mTOR mediate lipopolysaccharide-stimulated nitric oxide production in macrophages via interferon-beta. J Leukoc Biol. 2000;67:405-414
44. Carvalheiro T et al: Phenotypic and functional alterations on inflammatory peripheral blood cells after acute myocardial infarction. J Cardiovasc Transl Res. 2012;5:309-320
45. Sinfield JK et al: p38 MAPK alpha mediates cytokine-induced IL-6 and MMP-3 expression in human cardiac fibroblasts. Biochem Biophys Res Commun. 2013;430:419-424
46. Wrenger S et al: Down-regulation of T cell activation following inhibition of dipeptidyl peptidase IV/CD26 by the N-terminal part of the thromboxane A2 receptor. J Biol Chem. 2000;275:22180-22186
47. Kabashima K et al: Thromboxane A2 modulates interaction of dendritic cells and T cells and regulates acquired immunity. Nat Immunol. 2003;4:694-701
48. Dujardin KS et al: Prognostic value of a Doppler index combining systolic and diastolic performance in idiopathic-dilated cardiomyopathy. Am J Cardiol. 1998;82:1071-1076
49. Ascione L et al: Myocardial global performance index as a predictor of in-hospital cardiac events in patients with first myocardial infarction. J Am Soc Echocardiogr. 2003;16:1019-1023
50. Brusko TM, Wasserfall CH, Agarwal A, Kapturczak MH, Atkinson MA: An integral role for heme oxygenase-1 and carbon monoxide in maintaining peripheral tolerance by CD4+CD25+ regulatory T cells. J Immunol. 2005;174:5181-5186
51. Clark JE et al: Heme oxygenase-1-derived bilirubin ameliorates postischemic myocardial dysfunction. Am J Physiol Heart Circ Physiol. 2000;278:H643-H651
52. Basili S et al: Anoxia-reoxygenation enhances platelet thromboxane A2 production via reactive oxygen species-generated NOX2: effect in patients undergoing elective percutaneous coronary intervention. Arterioscler Thromb Vasc Biol. 2011;31:1766-1771
53. Nussinovitch U, Shoenfeld Y: Anti-troponin autoantibodies and the cardiovascular system. Heart. 2010;96:1518-1524
54. Kanellakis P, Dinh TN, Agrotis A, Bobik A: CD4(+)CD25(+) Foxp3(+) regulatory T cells suppress cardiac fibrosis in the hypertensive heart. J Hypertens. 2011;29:1820-1828

Peer reviewers: Zhiqiang Qu, PhD, Central Laboratory, Affiliated Hospital, Qingdao University, 16 Jiangsu Rd., Qingdao, China; Xiushan Wu, The Center for Heart Development, College of Life Science, Hunan Normal University, Changsha, 410081, Hunan Province, China;Erica C Campos Pulici, Laboratory of Cellular and Molecular Cardiology, Department of Pathology at the Ribeirão Preto Medical School, University of São Paulo, Av. Bandeirantes, 3900 - Monte Alegre, Ribeirão Preto, São Paulo, Brazil.